January - February 2020
ISSN: 0193 - 4120 Page No. 9666 - 9678

Unsteady Natural MHD Convection in Porous Medium Using Nonstandard Finite Difference Method

Zaihar Yaacob[1*], Mohammad Khatim Hasan[2] and Bahari Idrus[3]
[1]*Malaysian Institute of Chemical and Bioengineering Technology University Kuala Lumpur Malacca, Malaysia*
[2,3]*Centre for Artificial Intelligence Faculty of Information Science & Technology National University of Malaysia, Selangor, Malaysia*
zaihar@unikl.edu.my[1], mkh@ukm.edu.my[2],bahari@ukm.edu.my[3]

Article Info
Volume 82
Page Number: 9666 - 9678
Publication Issue:
January-February 2020

Article History
***Article Received**: 18 May 2019*
***Revised**: 14 July 2019*
***Accepted**: 22 December 2019*
***Publication**: 13 February 2020*

Abstract
Numerical solutions of unsteady magneto hydrodynamics convection in porous medium are the main concern of this paper. Isothermal walls with different temperatures are perpendicular to each other. The fluid inside the cavity generate heat non-uniformly and an incline magnetic field also gives effect to the fluid movement. Some new hybrid nonstandard finite difference schemes for unsteady problems are proposed. Overall, the new schemes improved the convergence rate up to 225 times faster and number of iteration up to 506 times less compared to classical finite difference scheme.

Keywords; *nonstandard finite difference method, magnetohydrodynamics, convection, porous cavity*

1. INTRODUCTION

One of the earliest experiments in two-dimensional porous space for unsteady heat convection was from [1] where vertical wall space is isothermic while horizontal wall is insulated. Changes in flow rates and isothermic contours are observed over time before equilibrium is reached in the system. Also studied is the influence of disparity in the ratio of height and width (also called aspect ratio).

In [2] studied the same problem as [1] by heating and temporarily cooling the elevated wall while the horizontal wall is adiabatic. In [3] performed an experimental analysis for the same problem as [2], which they used a rectangular cavity.

Darcy's Brinkmann-extended model was used by [4] to study unsteady actions in rectangular cavities interspersed with porous material. While, in [5] also conducted a rectangular porous cavity instability study. At the beginning, they analyzed the case of the steady-state ($t = 0$) with the left wall at T_h and the right wall at T_c where $T_h > T_c$ and the horizontal walls are adiabatic. Then at $t > 0$, the left vertical wall is suddenly heated to a temperature of $\bar{T}_h$ where $\bar{T}_h > T_h$ causes the flow field to become unsteady. Later [6] conducted similar experiments with fluid having differing temperatures in the cavity. Followed by [7] who studied unstable behavior with sinusoidal heated walls in porous cavity.

This paper explores the effects of sloping magnetic fields and non-uniform internal heating in rectangular porous cavity, combined with electrical current flow, on unsteady processes. The volatility of unsteady fluid flow with the magnetic field effect were investigated in [8-15].

In [16] studied the influence of the sloping magnetic field for the porous trapezoid cavity and in [17] continue it with the effect of a uniform internal heating. The results of non-uniform internal heating with opposite isothermal wall were then studied [18]-[19].

Thus the research in this paper focuses on the question of unsteady magneto hydrodynamics (MHD) with the effect of non-uniform internal heating on a perpendicular isothermal walls case which to our best knowledge is a new issue not addressed by either group. The most widely used numerical methods for solving the governing equations in porous medium unsteady behavior problems are the Finite difference methods (FDM) as in [4], [10-12], [1], [17]-[18]. Finite volume methods (FVM) in [5]-[6], [16-18].There are also the Differential Quadrature Method (DQM) by [15], and one-dimensional analytical methods [8]-[9], as well as the nonstandard finite difference method by [19], [26].

More recently [20-22] have applied the Spectral Fourier Galerkin (SFG) approach to the problem of instability in the porous cavity. By contrast, SFG produces results are similar to the advanced finite element method (FEM) but SFG has the advantage of being efficient at faster convergence rates and less CPU time. Therefore, the SFG is considered as a new benchmark method for natural convection in porous cavity problem.

There was not much work on the unsteady MHD problem with non-uniform internal heating effects. Consequently, the results of this study are useful to understand the properties of MHD convection in porous medium or more complex problems. This research may also test the efficacy of the current NSFD scheme in addressing the said problem.

2. PROBLEM FORMULATION

Unsteady natural convection in a rectangular cavity coupled to a porous medium flow through electrical current and contains a uniform internal heat generator is considered here. The cavity is saturated by a uniform sloping magnetic field (see Fig. 1)

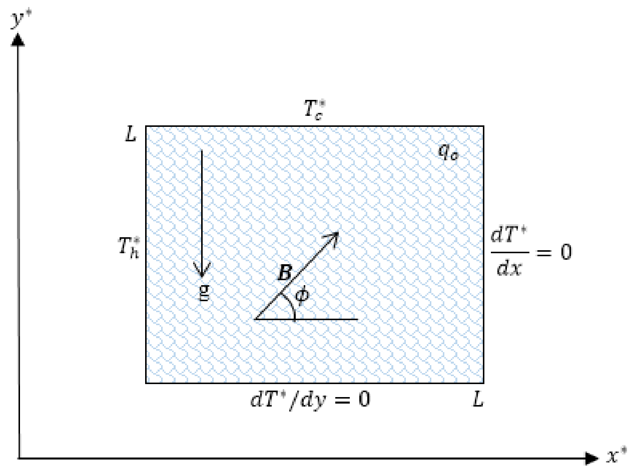

Figure 1. Rectangular cavity saturated with porous medium

The governing equations for the problem of unsteady MHD problems are as in equation (1)-(6) [17]:

$$\nabla \cdot \boldsymbol{V}^* = 0\,, \tag{1}$$

$$\boldsymbol{V}^* = \frac{K}{\mu}(-\nabla P^* + \rho\mathbf{g} + \boldsymbol{J}\times\boldsymbol{B})\,, \tag{2}$$

$$\frac{\partial T^*}{\partial t^*} + (\boldsymbol{V}^*\cdot\nabla)T^* = \alpha_m\nabla^2 T^* + \frac{q_o}{\rho_0 c_p}(T^* - T_c^*)^p\,, \tag{3}$$

$$\nabla \cdot \boldsymbol{J} = 0\,, \tag{4}$$

$$\boldsymbol{J} = \sigma(-\nabla\varphi + \boldsymbol{V}^*\times\boldsymbol{B})\,, \tag{5}$$

$$\rho = \rho_0[1 - \beta(T^* - T_c^*)]\,. \tag{6}$$

where $\boldsymbol{V}^*$ is the velocity vector, P^* is the fluid pressure, $\boldsymbol{J}$ **i**s an electric current vector, φ is an electric potential, $\mathbf{g}$ isa gravitational acceleration vector, K is the permeability of the porous medium, α_m is an effective thermal diffusivity, $\boldsymbol{B}$ is an external magnetic field, ρ is the fluid density, T^* is the fluid temperature, μ is the dynamic viscosity, β is the coefficient of thermal expansion, q_0 is an internal heat generation, p is an internal heat generation exponent, c_p is a specific heat at constant pressure, σ is an electrical conductivity, ρ_0 is a reference fluid density, $-\nabla\varphi$ is an associated electric field and t^* is the time. Equation (4)-(5) can be reduced to $\nabla^2\varphi = 0$ as described in [8]. Unique solution for that equation is $\nabla\varphi = 0$ since there is always an electrically insulating boundary around the enclosure. Thus, it follows that the electric field vanishes everywhere. Therefore, equation(1) – (3) in two dimensions are:

$$\frac{\partial u^*}{\partial x^*} + \frac{\partial v^*}{\partial y^*} = 0\,, \tag{7}$$

$$u^* = -\frac{K}{\mu}\left(\frac{\partial P^*}{\partial x^*} + \rho_0\big(1 - \beta(T^* - T_c^*)\big)\mathbf{g}sin\gamma \right. \\ \left. + \sigma B_0^2(v^* sin\phi cos\phi - u^* \sin^2\phi)\right), \tag{8}$$

$$v^* = -\frac{K}{\mu}\left(\frac{\partial P^*}{\partial y^*} + \rho_0\big(1 - \beta(T^* - T_c^*)\big)\mathbf{g}\cos\gamma \right. \\ \left. + \sigma B_0^2(u^* sin\phi cos\phi - v^* sin^2\phi)\right), \tag{9}$$

$$\frac{\partial T^*}{\partial t^*} + u^*\frac{\partial T^*}{\partial x^*} + v^*\frac{\partial T^*}{\partial y^*} = \alpha_m\left(\frac{\partial^2 T^*}{\partial x^{*2}} + \frac{\partial^2 T^*}{\partial x^{*2}}\right) + \frac{q_o}{\rho_0 c_p}(T^* - T_c^*)^p \tag{10}$$

where B_0 is the magnitude of B and γ is the inclined angle of the cavity which takes zero value for vertical cavity. The boundary conditions are:

$$\begin{array}{llll} x^* = L\,, & u^*, v^* = 0\,, & \dfrac{\partial T^*}{\partial y^*} = 0 & (0 < y^* < L), \\ x^* = 0\,, & u^*, v^* = 0\,, & T^* = T_h^*(0 < y^* < L), & \\ y^* = L\,, & u^*, v^* = 0\,, & T^* = T_c^*(0 < x^* < L), & \\ y^* = 0\,, & u^*, v^* = 0\,, & \dfrac{\partial T^*}{\partial x^*} = 0 & (0 < x^* < L). \end{array} \tag{11}$$

Eliminating the pressure terms from equation (8)-(9) in the usual way, to get equation (12):

$$\frac{\partial u^*}{\partial y^*} - \frac{\partial v^*}{\partial x^*} = \frac{-K\beta \mathrm{g}}{\nu}\frac{\partial T^*}{\partial x^*} + \frac{\sigma K B_0^2}{\mu} \\ \times\left(-\frac{\partial u^*}{\partial y^*}\sin^2\phi + 2\frac{\partial v^*}{\partial y^*} sin\phi cos\phi + \frac{\partial v^*}{\partial x^*}\cos^2\phi\right), \tag{12}$$

where $\nu = \mu/\rho_0$ is the kinematic viscosity of the fluid. Then, using the following dimensionless parameters:

$$x = \frac{x^*}{L} \ \ , \ y = \frac{y^*}{L} \ \ , \ u = \frac{L}{\alpha_m} u^* \ , \ v = \frac{L}{\alpha_m} v^* \ \ , \ \theta = \frac{T^* - T_c^*}{\Delta T} \ \ , \quad t = \frac{\alpha_m}{L^2} t^* \, , \qquad \Delta T = T_h^* - T_c^* \, . \tag{13}$$

The stream function are defined as $u = \partial\psi/\partial y$ dan $v = -\partial\psi/\partial x$, and when substituted into equation (10) and (13) we have the dimensionless equation (14)-(15) with the corresponding boundary conditions in equation(16):

$$\frac{\partial\theta}{\partial t} + \frac{\partial\psi}{\partial y}\frac{\partial\theta}{\partial x} - \frac{\partial\psi}{\partial x}\frac{\partial\theta}{\partial y} = \frac{\partial^2\theta}{\partial x^2} + \frac{\partial^2\theta}{\partial y^2} + G\theta^p , \tag{14}$$

$$\frac{\partial^2\psi}{\partial x^2} + \frac{\partial^2\psi}{\partial y^2} = -Ra\frac{\partial\theta}{\partial x} - Ha^2\left(\frac{\partial^2\psi}{\partial y^2} sin^2\,\phi + 2\frac{\partial^2\psi}{\partial x\partial y} sin\phi cos\phi + \frac{\partial^2\psi}{\partial x^2} cos^2\,\phi\right), \tag{15}$$

$$\begin{aligned} &x = L \ , \quad u, v = 0 \ , \quad \frac{\partial\theta}{\partial y} = 0 \quad (0 < y < L), \\ &x = 0 \ , \quad u, v = 0 \ , \quad \theta = 1 \quad (0 < y < L), \\ &y = L \ , \quad u, v = 0 \ , \quad \theta = 0 (0 < x < L), \\ &y = 0 \ , \quad u, v = 0 \ , \quad \frac{\partial\theta}{\partial x} = 0 \quad (0 < x < L). \end{aligned} \tag{16}$$

where $Ra = -K\beta\mathbf{g}\mathrm{L}\Delta\mathrm{T}/\alpha_m\nu$ is the Rayleigh number, $G = q_o L^2(\Delta T)^{p-1}$ is an internal heat generator coefficient and $(Ha)^2 = \sigma K B_0^2/\mu$ is the Hartmann number to represent magnetic field effect. In equation (15), $\phi = 0$ implies horizontal magnetic field direction and $\phi = \pi/2$ is for vertical magnetic field.

Once the temperature distribution inside the region is known, the heat flow rate of each hot and cold wall can be calculated using the average Nusselt number $\overline{Nu}_h = \int_0^1 (\partial\theta/\partial x)_{x=0}$ at the hot wall and $\overline{Nu}_c = \int_0^1 (\partial\theta/\partial y)_{y=1}\, dy$ at the cold wall.

3. NUMERICAL METHODS AND VALIDATION

The pseudo-transient technique took a long time to converge and fails to converge for large Ha values $(Ha > 5)$. For this reason, the unsteady equation (14) is solve using the alternating direction implicit (ADI) while the steady equation (15) is by using the Gauss-Seidel (GS) iteration method [17].Finite difference scheme for equation(14) is:

$$\left(\frac{\partial^2\theta}{\partial x^2} + \frac{\partial^2\theta}{\partial y^2} - \frac{\partial\theta}{\partial t}\right)_{i,j} = (S_\theta)_{i,j} \, , \tag{17}$$

where

January - February 2020
ISSN: 0193 - 4120 Page No. 9666 - 9678

$$(S_\theta)_{i,j} = \left(\frac{\partial\psi}{\partial y}\frac{\partial\theta}{\partial x}\right)_{i,j} - \left(\frac{\partial\psi}{\partial x}\frac{\partial\theta}{\partial y}\right)_{i,j} - G(\theta^p)_{i,j}. \tag{18}$$

And the discrete form for equation(17) are in two stages:

$$\frac{\theta_{i+1,j}^{k+\frac{1}{2}} - 2\theta_{i,j}^{k+\frac{1}{2}} + \theta_{i-1,j}^{k+\frac{1}{2}}}{(\Delta x)^2} + \frac{\theta_{i,j+1}^{k} - 2\theta_{i,j}^{k} + \theta_{i,j-1}^{k}}{(\Delta y)^2} - \left(\frac{\theta_{i,j}^{k+\frac{1}{2}} - \theta_{i,j}^{k}}{\Delta t}\right) = (S_\theta)_{i,j}\ , \tag{19}$$

$$\frac{\theta_{i+1,j}^{k+\frac{1}{2}} - 2\theta_{i,j}^{k+\frac{1}{2}} + \theta_{i-1,j}^{k+\frac{1}{2}}}{(\Delta x)^2} + \frac{\theta_{i,j+1}^{k+1} - 2\theta_{i,j}^{k+1} + \theta_{i,j-1}^{k+1}}{(\Delta y)^2} - \left(\frac{\theta_{i,j}^{k+1} - \theta_{i,j}^{k+\frac{1}{2}}}{\Delta t}\right) = (S_\theta)_{i,j} \tag{20}$$

Equation (19)-(20) are simplified by multiplying with Δt and rearranged to get equation (21)-(22):

$$r_x\theta_{i+1,j}^{k+\frac{1}{2}} - (1+2r_x)\theta_{i,j}^{k+\frac{1}{2}} + r_x\theta_{i-1,j}^{k+\frac{1}{2}} = -r_y\theta_{i,j+1}^{k} - (1-2r_y)\theta_{i,j}^{k} - r_y\theta_{i,j-1}^{k} + (\Delta t)(S_\theta)_{i,j}\ , \tag{21}$$

$$r_y\theta_{i,j+1}^{k+1} - (1+2r_y)\theta_{i,j}^{k+1} + r_y\theta_{i,j-1}^{k+1} = -r_x\theta_{i+1,j}^{k+\frac{1}{2}} - (1-2r_x)\theta_{i,j}^{k+\frac{1}{2}} - r_x\theta_{i-1,j}^{k+\frac{1}{2}} + (\Delta t)(S_\theta)_{i,j}\ , \tag{22}$$

where

$$r_x = \frac{\Delta t}{(\Delta x)^2}\ , r_y = \frac{\Delta t}{(\Delta y)^2} \tag{23}$$

and k is the iteration level.Gauss-Seidel scheme for equation(15) is:

$$\left(\frac{\partial^2\psi}{\partial x^2} + \frac{\partial^2\psi}{\partial y^2}\right)_{i,j} = \left(S_\psi\right)_{i,j}, \tag{24}$$

where

$$\left(S_\psi\right)_{i,j} = -Ra\left(\frac{\partial\theta}{\partial x}\right)_{i,j} - \left(SA_\psi\right)_{i,j}, \tag{25}$$

and

$$\left(SA_{\psi}\right)_{i,j} = Ha^2\left(\left(\frac{\partial^2\psi}{\partial y^2}\right)_{i,j} sin^2\phi + 2\left(\frac{\partial^2\psi}{\partial x\partial y}\right)_{i,j} sin\phi cos\phi + \left(\frac{\partial^2\psi}{\partial x^2}\right)_{i,j} cos^2\phi\right). \tag{26}$$

Discrete form for equation(24):

$$\frac{\psi_{i+1,j} - 2\psi_{i,j} + \psi_{i-1,j}}{(\Delta x)^2} + \frac{\psi_{i,j+1} - 2\psi_{i,j} + \psi_{i,j-1}}{(\Delta y)^2} = \left(S_{\psi}\right)_{i,j}, \tag{27}$$

Equation (27) is simplified following the successive over-relaxation (SOR) technique:

$$\psi_{i,j} = (1-\omega)\psi_{i,j} + \frac{\omega}{2(1+B^2)}\left[\psi_{i+1,j} - 2\psi_{i,j} + \psi_{i-1,j} - \Delta x\left(S_{\psi}\right)_{i,j}\right], \tag{28}$$

where $B = \Delta x/\Delta y$, and $1 < \omega < 2$ is the relaxation factor. But, for Gauss-Seidel iteration $\omega = 1$.Equation (21)-(22), and (28) are then solve iteratively until the following convergence criteria is achieve.

$$\frac{\sum_{i,j}\left|\Gamma_{i,j}^{n+1} - \Gamma_{i,j}^{n}\right|}{\sum_{i,j}\left|\Gamma_{i,j}^{n+1}\right|} \leq \varepsilon \tag{29}$$

where Γ is ψ or θ, n is the iteration number and ε is the convergence factor set as $\varepsilon = 10^{-5}$.

To verify the computational code, a precision test was performed for the values of $Ra = 10, 10^2$ and 10^3 for the case of $Ha = G = p = \theta = 0$. Average Nusselt numbers at the hot wall $(\overline{Nu}_h)$and cold wall $(\overline{Nu}_c)$ were calculated and compared with results by previous researchers for the isothermal wall problem as shown in Table 1. It is clear from the values in the table that the code used produces equivalent results as other researchers. Some fluid flow diagrams and temperature distributions for different time intervals are also compared with [23] as shown in Figure 2-5. Notably, the temperature distribution obtained in this analysis is identical to It is noteworthy that the temperature distribution obtained in this study is similar to [23]. The results presented so far provide the assurance that the techniques used in this study are good and appropriate for the perpendicular isothermal wall problems.

January - February 2020
ISSN: 0193 - 4120 Page No. 9666 - 9678

Table 1. Comparison of $\overline{Nu}_h$ and $\overline{Nu}_c$ values with other researches for perpendicular isothermal walls $(Ra = 100,\ Ha = G = p = \theta = 0)$

Reference	Mesh Size	$\overline{Nu}_h$	$\overline{Nu}_c$
[17], FDM	26 x 26	8.2636	8.224
	51 x 51	9.2162	9.2008
	101 x 101	10.1319	10.1247
	R.E.	10.4371	10.4326
[23], FDM	26 x 26	8.5553	8.2786
	51 x 51	9.3885	9.2271
	101 x 101	10.2297	10.1383
This paper, NSFD	26 x 26	8.4334	8.1606
	51 x 51	9.3266	9.1637
	101 x 101	10.1993	10.1048

Table 2. New NSFD-H schemes

Scheme	Space,Δx& Δy	Time,Δt
FDM	$\Delta x = 1/Nx$, $\Delta y = 1/Ny$	$\Delta t = 1/Nt$
NSFD-H1	$\Delta x \to e^{\Delta x} - 1$; $\Delta y = \Delta x$	$\Delta t = \Delta x$
NSFD-H2	$\Delta x \to 2\sinh\left(\frac{\Delta x}{2}\right)$; $\Delta y = \Delta x$	$\Delta t = \Delta x$

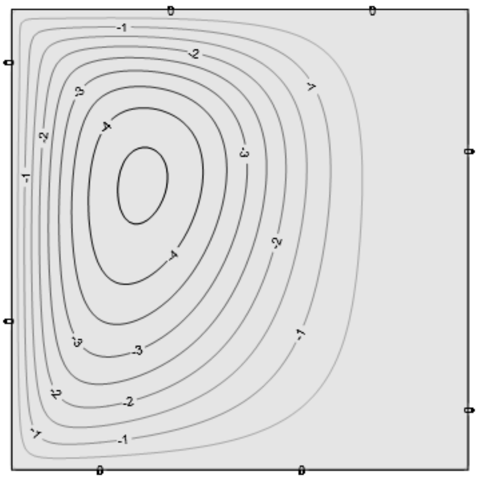

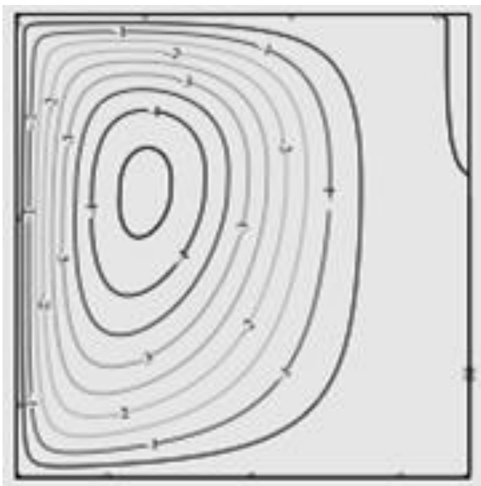

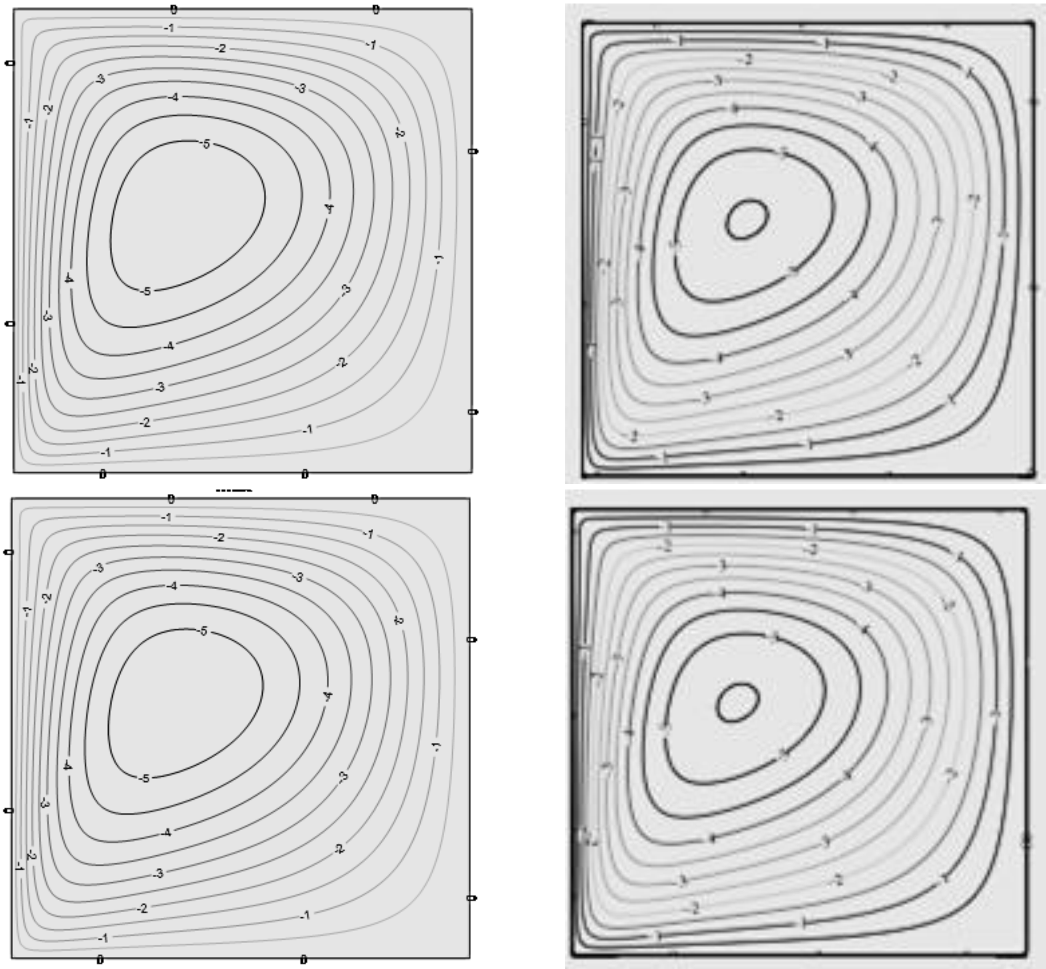

Figure 2. Streamline comparison between this study (left) with [23] (right) for $Nx = 101$. From top, $t = 0.1, 0.5, 0.8$ seconds

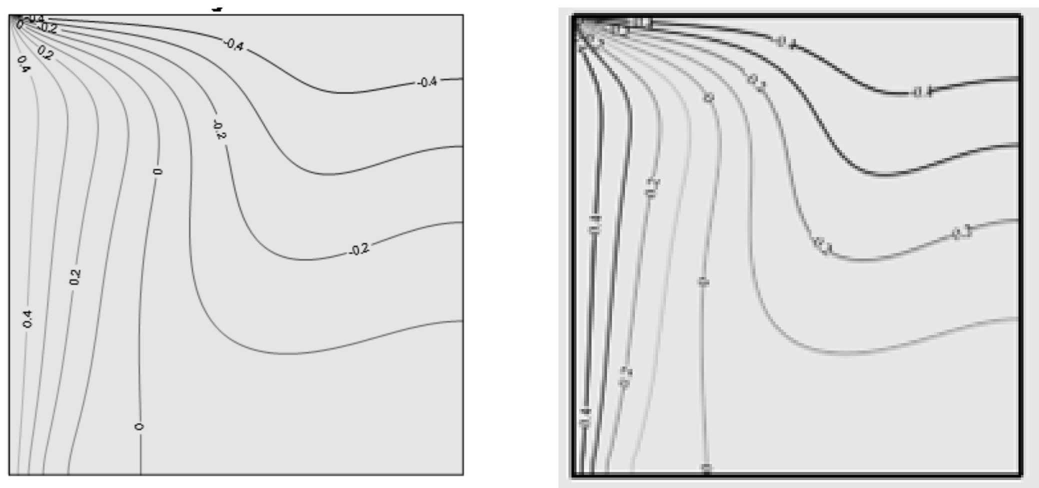

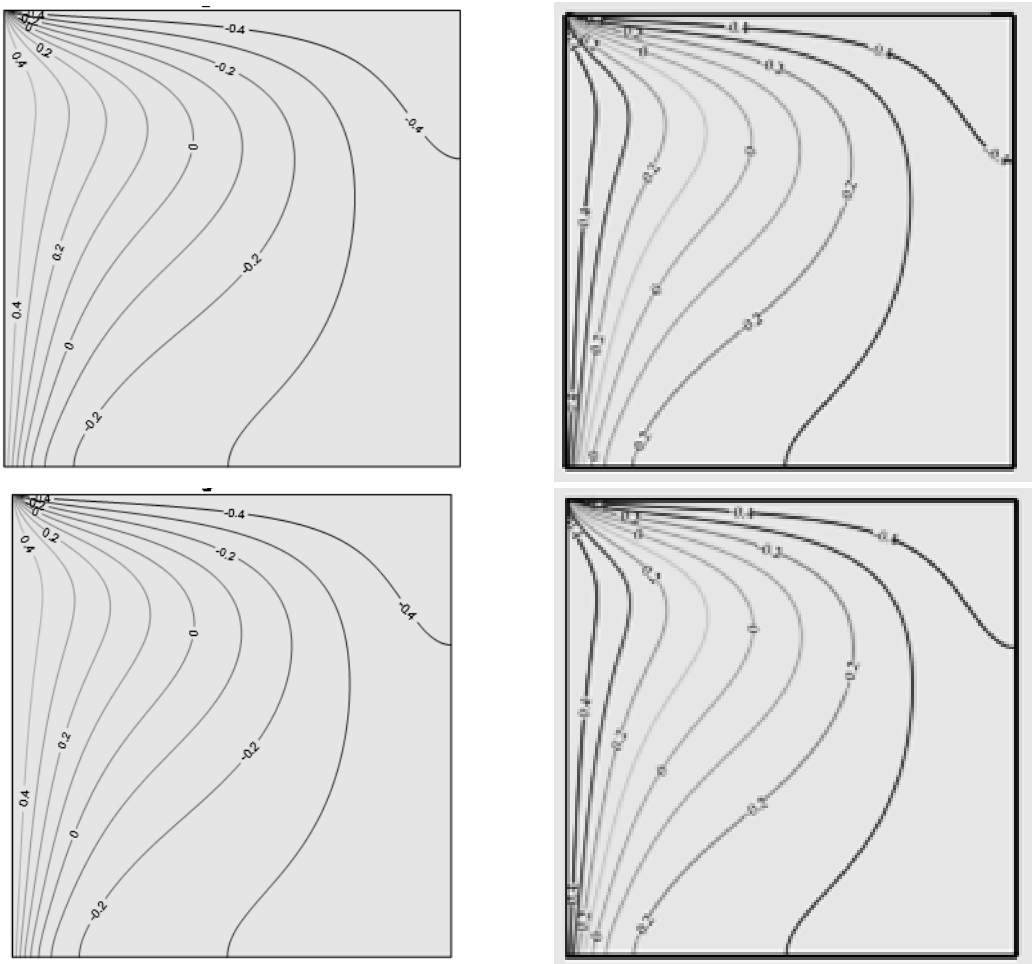

Figure 3. Isotherm comparison between this study (left) with [23] (right) for $Nx = 101$. From top, $t = 0.1, 0.5, 0.8$ seconds

TEST Engineering & Management
January - February 2020
ISSN: 0193 - 4120 Page No. 9666 - 9678

The finite difference method (FDM) requires the step size $h(\Delta x, \Delta y)$ are sufficiently small $(h \ll 0.1)$ to get good results. This causes the program to take a long time with a large number of iterations to get a meaningful result. For example, when a program is run with a grid size of 1 / h = 200, the convergence time exceeds 20 minutes and the number of iterations approaches 100,000.

Studies by [24]-[25] explains the role of nonstandard finite difference method (NSFD) in solving the problem of instability in ordinary differential equations (ODE) and partial differential equations (PDE) when standard finite difference method (FDM) was used. But what about the speed to find a solution to the problem? In addition to stability, the effectiveness of a new scheme can also be determined by the precision and speed of the solution. A complex problem such as MHD requires accurate solution that will take a very long time to converge. In this regard, this paper introduces several non-standard finite difference schemes aimed at testing the effectiveness of NSFD compared to FDM. The proposed scheme consists of combination between space (Δx) and time (Δt) functions and we call it as NSFD hybrid (NSFD-H) schemes (see Table 2). This comes from the observation of several studies by [24]-[25] which states that a finite difference scheme must have a relationship between the space and time interval, i.e. ($\Delta t \equiv \Delta x$.

4. RESULTS AND DISCUSSION

Results between FDM and NSFD-H is refered in Table 3-4 for the values of $\overline{Nu}_h$ and $\overline{Nu}_c$. All values are for the cases $Ra = 10, 10^3, Ha = 5, G = 3, p = 3,\ \phi = 0$ and various Nx. Clearly can be seen that NSFD-H scheme has good accuracy and is comparable to the FDM scheme.

Comparison of convergence time and number of iterations can be found in Table 5 and Table 6. It is calculated by dividing the FDM value by the NSFD-H value, and the results we call as multiplier difference (MD). Table 5 shows the MD convergence time, that clearly shown the NSFD-H scheme improve the convergence time between 7.20 and 178.31 times faster than FDM. The number of iterations taken as shown in Table 6, also shows that NSFD-H reduced the number of iterations by 7.64 to 506.35 times less compared to FDM. So it is clear that NSFD-H schemes has much better efficiency than the FDM for small Nx values (4, 6, 8,…, 50), but at the same time maintain its accuracy.

5. CONCLUSION

In this paper, the problem of instability in the porous cavity with non-uniform internal heating effects and sloping magnetic field effects is solved numerically. The isothermic walls are adjacent or perpendicular which is heated on the left and cooled at the top. Several new NSFD-H schemes are applied in solving the governing equations. All the schemes succeeded in reducing the convergence time and number of iterations compared to the FDM scheme while maintaining accuracy. The convergence time is accelerated up to 225 times while the number of iterations reduced up to 506 fold. Therefore, the study in this paper has shown that the NSFD-H schemes is much more efficient than the FDM scheme for Nx values between 4 and 50.

Table 3.$\overline{Nu}_h$absolute difference between FDM dan NSFD-H

|FDM – NSFD-H|			
Ra	Nx	H1	H2
10	4	2.85E-05	0.001203
	6	0.002216	0.000357
	8	0.001832	0.001007
	10	0.0025	0.000279
	20	0.001792	0.000194
	30	0.001407	7.01E-05
	40	0.001143	2.64E-05
	50	0.000961	4.89E-06
10^3	4	0.296398	0.036296

Published by: The Mattingley Publishing Co., Inc.

January - February 2020
ISSN: 0193 - 4120 Page No. 9666 - 9678

	6	0.260143	0.017734
	8	0.222348	0.003409
	10	0.205459	0.011841
	20	0.11172	0.004879
	30	0.07184	0.001167
	40	0.052642	0.000109
	50	0.041995	0.000145

Table 4. $\overline{Nu}_c$ absolute difference between FDM dan NSFD-H

|FDM – NSFD-H|			
Ra	Nx	H1	H2
10	4	0.004848	0.001272
	6	0.004351	0.000431
	8	0.00477	0.001049
	10	0.003739	0.000321
	20	0.002445	0.000206
	30	0.001708	7.68E-05
	40	0.001309	3.08E-05
	50	0.001058	8.07E-06
10^3	4	0.01768	0.012508
	6	0.10535	0.003763
	8	0.129669	0.000953
	10	0.125498	0.001865
	20	0.0819	0.000677
	30	0.056974	6.45E-05
	40	0.043343	8.96E-05
	50	0.03487	3.27E-05

Table 5. MD convergence time between FDM and NSFD-H

FDM / NSFD-H			
Ra	Nx	H1	H2
10	4	40.34622	34.66879
	6	178.3068	165.2156
	8	94.1423	124.2407
	10	143.8129	131.7302
	20	56.71737	53.45134
	30	28.94423	30.9454
	40	15.54858	19.92512
	50	16.89483	14.94922
10^3	4	32.3387	34.36835
	6	176.9254	173.7936
	8	130.3712	174.8612
	10	108.9441	103.3307
	20	29.98366	33.61304
	30	16.23907	16.88848
	40	20.50993	13.60933
	50	7.202614	7.573697

Table 6. MD number of iterations between FDM and NSFD-H

FDM / NSFD-H			
Ra	Nx	H1	H2
10	4	324.314	303.163
	6	282.4422	271.366
	8	163.1327	158.2871
	10	164.7564	161.2384
	20	61.75215	60.49038
	30	31.44884	33.73855
	40	16.68327	21.60588
	50	18.0422	15.87766
10^3	4	506.3529	461.1429
	6	341.8125	317.9651
	8	256.6138	235.5
	10	136.2388	137.608
	20	32.30588	36.88156
	30	17.93287	18.63721
	40	21.58742	14.67673
	50	7.641594	8.129702

ACKNOWLEDGMENTS

Authors gratefully acknowledge the financial support received from UNIKL, MARA and from research grant GGP-2017-023.

REFERENCES

[1] Poulikakos, D. and Bejan, A., 1983. Unsteady natural convection in a porous layer. The Physics of Fluids, 26(5), pp.1183-1191.

[2] Saeid, N.H. and Pop, I., 2004. Transient free convection in a square cavity filled with a porous

medium. International Journal of Heat and Mass Transfer, 47(8-9), pp.1917-1924.
[3] Aldabbagh, L.Y. and Manesh, H.F., 2008. Unsteady natural convection inside a porous enclosure heated from the side. Journal of Porous Media, 11(1), pp. 73-83.
[4] Pakdee, W. and Rattanadecho, P., 2009. Numerical analysis of natural convection in porous cavities with partial convective cooling conditions. Journal of Porous Media, 12(11), pp. 1083-1100.
[5] Kumari, M. and Nath, G., 2009. Unsteady natural convection flow in a square cavity filled with a porous medium due to impulsive change in wall temperature. Transport in Porous Media, 77(3), pp.463-474.
[6] Kumari, M. and Nath, G., 2014. Transient natural convection flow in a rectangular cavity filled with a porous material with localized heating from below and thermal stratification. Journal of Porous Media, 17(7), pp. 647-655.
[7] Sojoudi, A., Saha, S.C., Khezerloo, M. and Gu, Y.T., 2014. Unsteady natural convection within a porous enclosure of sinusoidal corrugated side walls. Transport in Porous Media, 104(3), pp.537-552.
[8] Garandet, J.P., Alboussiere, T. and Moreau, R., 1992. Buoyancy driven convection in a rectangular enclosure with a transverse magnetic field. International Journal of Heat and Mass Transfer, 35(4), pp.741-748.
[9] Mahmud, S., Tasnim, S.H. and Mamun, M.A.H., 2003. Thermodynamic analysis of mixed convection in a channel with transverse hydromagnetic effect. International Journal of Thermal Sciences, 42(8), pp.731-740.
[10] Hossain, M.A., Hafiz, M.Z. and Rees, D.A.S., 2005. Buoyancy and thermocapillary driven convection flow of an electrically conducting fluid in an enclosure with heat generation. International Journal of Thermal Sciences, 44(7), pp.676-684.
[11] Chamkha, A.J. and Al-Naser, H., 2002. Hydromagnetic double-diffusive convection in a rectangular enclosure with uniform side heat and mass fluxes and opposing temperature and concentration gradients. International Journal of Thermal Sciences, 41(10), pp.936-948.
[12] Alchaar, S., Vasseur, P. and Bilgen, E., 1995. Hydromagnetic natural convection in a tilted rectangular porous enclosure. Numerical Heat Transfer, Part A: Applications, 27(1), pp.107-127.
[13] Ramambason, D.R. and Vasseur, P., 2007. Influence of a magnetic field on natural convection in a shallow porous enclosure saturated with a binary fluid. Acta Mechanica, 191(1-2), pp.21-35.
[14] Zeng, M., Wang, Q., Ozoe, H., Wang, G. and Huang, Z., 2009. Natural convection of diamagnetic fluid in an enclosure filled with porous medium under magnetic field. Progress in Computational Fluid Dynamics, an International Journal, 9(2), pp.77-85.
[15] Ece, M.C. and Büyük, E., 2006. Natural-convection flow under a magnetic field in an inclined rectangular enclosure heated and cooled on adjacent walls. Fluid Dynamics Research, 38(8), pp.564-590.
[16] Saleh, H., Roslan, R. and Hashim, I., 2011. Natural convection in a porous trapezoidal enclosure with an inclined magnetic field. Computers & Fluids, 47(1), pp.155-164.
[17] Revnic, C., Grosan, T., Pop, I. and Ingham, D.B., 2011. Magnetic field effect on the unsteady free convection flow in a square cavity filled with a porous medium with a constant heat generation. International Journal of Heat and Mass Transfer, 54(9-10), pp.1734-1742.
[18] Saleh, H. and Hashim, I., 2012. Hydromagnetic natural convection flow in a fluid-saturated porous medium with nonuniform heat generation. Advances in Mechanical Engineering, 4, pp. 1-13.
[19] Moaddy, K., Hashim, I. and Saleh, H., 2012. A non-standard finite difference scheme for convection in a porous cavity. Journal of Difference Equations and Applications, 18(3), pp.461-469.
[20] Amin, F. and Malek, A., 2017. Spectral Fourier–Galerkin benchmark solution for natural convection in an inclined saturated porous medium. Numerical Heat Transfer, Part B: Fundamentals, 71(4), pp.372-395.
[21] Fahs, M., Younes, A. and Mara, T.A., 2014. A new benchmark semi-analytical solution for

density-driven flow in porous media. Advances in Water Resources, 70, pp.24-35.

[22] Fahs, M., Younes, A. and Makradi, A., 2015. A reference benchmark solution for free convection in a square cavity filled with a heterogeneous porous medium. Numerical Heat Transfer, Part B: Fundamentals, 67(5), pp.437-462.

[23] Selamat, M.S., Hashim, I. and Hasan, M.K., 2012. Transient natural convection in porous square cavity heated and cooled on adjacent walls. Mathematical Problems in Engineering, 2012, pp. 1-10.

[24] Mickens, R.E., 1994. A best finite-difference scheme for the fisher equation. Numerical Methods for Partial Differential Equations, 10(5), pp.581-585.

[25] Mickens, R.E., 2000. Analysis of a finite-difference scheme for a linear advection-diffusion-reaction equation. Journal of Sound and Vibration, 5(236), pp.901-903.

[26] Yaacob, Z. and Hasan, M.K., 2015. Nonstandard finite difference schemes for natural convection in an inclined porous rectangular cavity. IEEEInternational Conference on Electrical Engineering and Informatics, pp. 665-669.